

Hydrocarbon Synthesis from Carbon Dioxide and Hydrogen: A Two-Step Process

David M Drab, Heather D Willauer, Matthew T Olsen, Ananth Ramagopal, George W. Mushrush, Jeffrey W Baldwin, Dennis R Hardy, and Frederick W Williams

Energy Fuels, **Just Accepted Manuscript** • DOI: 10.1021/ef4011115 • Publication Date (Web): 14 Aug 2013

Downloaded from <http://pubs.acs.org> on August 19, 2013

Just Accepted

"Just Accepted" manuscripts have been peer-reviewed and accepted for publication. They are posted online prior to technical editing, formatting for publication and author proofing. The American Chemical Society provides "Just Accepted" as a free service to the research community to expedite the dissemination of scientific material as soon as possible after acceptance. "Just Accepted" manuscripts appear in full in PDF format accompanied by an HTML abstract. "Just Accepted" manuscripts have been fully peer reviewed, but should not be considered the official version of record. They are accessible to all readers and citable by the Digital Object Identifier (DOI®). "Just Accepted" is an optional service offered to authors. Therefore, the "Just Accepted" Web site may not include all articles that will be published in the journal. After a manuscript is technically edited and formatted, it will be removed from the "Just Accepted" Web site and published as an ASAP article. Note that technical editing may introduce minor changes to the manuscript text and/or graphics which could affect content, and all legal disclaimers and ethical guidelines that apply to the journal pertain. ACS cannot be held responsible for errors or consequences arising from the use of information contained in these "Just Accepted" manuscripts.



ACS Publications
High quality. High impact.

Energy & Fuels is published by the American Chemical Society, 1155 Sixteenth Street N.W., Washington, DC 20036

Published by American Chemical Society. Copyright © American Chemical Society. However, no copyright claim is made to original U.S. Government works, or works produced by employees of any Commonwealth realm Crown government in the course of their duties.

Report Documentation Page				Form Approved OMB No. 0704-0188	
Public reporting burden for the collection of information is estimated to average 1 hour per response, including the time for reviewing instructions, searching existing data sources, gathering and maintaining the data needed, and completing and reviewing the collection of information. Send comments regarding this burden estimate or any other aspect of this collection of information, including suggestions for reducing this burden, to Washington Headquarters Services, Directorate for Information Operations and Reports, 1215 Jefferson Davis Highway, Suite 1204, Arlington VA 22202-4302. Respondents should be aware that notwithstanding any other provision of law, no person shall be subject to a penalty for failing to comply with a collection of information if it does not display a currently valid OMB control number.					
1. REPORT DATE 19 AUG 2013		2. REPORT TYPE		3. DATES COVERED 00-00-2013 to 00-00-2013	
4. TITLE AND SUBTITLE Hydrocarbon Synthesis from Carbon Dioxide and Hydrogen: A Two-Step Process				5a. CONTRACT NUMBER	
				5b. GRANT NUMBER	
				5c. PROGRAM ELEMENT NUMBER	
6. AUTHOR(S)				5d. PROJECT NUMBER	
				5e. TASK NUMBER	
				5f. WORK UNIT NUMBER	
7. PERFORMING ORGANIZATION NAME(S) AND ADDRESS(ES) US Naval Research Laboratory, 4555 Overlook Avenue, SW, Washington, DC, 20375				8. PERFORMING ORGANIZATION REPORT NUMBER	
9. SPONSORING/MONITORING AGENCY NAME(S) AND ADDRESS(ES)				10. SPONSOR/MONITOR'S ACRONYM(S)	
				11. SPONSOR/MONITOR'S REPORT NUMBER(S)	
12. DISTRIBUTION/AVAILABILITY STATEMENT Approved for public release; distribution unlimited					
13. SUPPLEMENTARY NOTES Energy & Fuels					
14. ABSTRACT					
15. SUBJECT TERMS					
16. SECURITY CLASSIFICATION OF:			17. LIMITATION OF ABSTRACT Same as Report (SAR)	18. NUMBER OF PAGES 18	19a. NAME OF RESPONSIBLE PERSON
a. REPORT unclassified	b. ABSTRACT unclassified	c. THIS PAGE unclassified			

Hydrocarbon Synthesis from Carbon Dioxide and Hydrogen: A Two-Step Process

David M. Drab¹, Heather D. Willauer^{2*}, Matthew T. Olsen¹, Ramagopal Ananth³, George W. Mushrush², Jeffrey W. Baldwin⁴, Dennis R. Hardy⁵, and Frederick W. Williams⁶

¹NRC Postdoctoral Research Associate, Materials Science & Technology Division, Code 6300.2, US Naval Research Laboratory, 4555 Overlook Avenue, SW, Washington, DC, 20375, ²Materials Science & Technology Division, Code 6300.2, US Naval Research Laboratory, Washington, DC 20375, ³Chemistry Division, Code 6185, Naval Research Laboratory, Washington, DC, 20375, ⁴Acoustics Division, Code 7136, Naval Research Laboratory, Washington, DC, 20375, ⁵Nova Research Inc., 1900 Elkin Street, Alexandria, VA 22308, ⁶Chemistry Division, Code 6104, Naval Research Laboratory, Washington, DC, 20375

Abstract

CO₂ hydrogenation to olefins and ethylene oligomerization was investigated in efforts to improve catalyst composition and reaction conditions needed for scale-up. The hydrogenation of CO₂ to hydrocarbons is investigated over γ -alumina-supported iron-based catalysts modified with manganese and potassium promoters and a silica-stabilized coating under fixed-bed reactor conditions to produce unsaturated hydrocarbons as feedstock chemicals for jet fuel synthesis. The stabilizer is introduced by impregnating the K/Mn/Fe on Al₂O₃ catalyst with tetraethylorthosilicate (TEOS) to minimize the deactivating effects of water on catalyst activity in CO₂ hydrogenation. The K/Mn/Fe on Al₂O₃ catalyst modified with the TEOS and reduced in CO produced a lighter end fraction of olefins compared with the catalyst reduced in H₂. To increase the chain length of the olefins formed in the CO₂ hydrogenation step, investigation of oligomerization reaction is conducted in a separate experiment, where pure ethylene is used as a model olefin. Ethylene oligomerization over pelletized amorphous silica-alumina (ASA)-supported Ni catalysts demonstrated high conversion and selectivity towards the jet fuel fraction (C8-C16) at very low MHSV.

Keywords: CO₂ hydrogenation; fixed-bed reactor, olefin/paraffin ratio; GHSV (gas hourly space velocity), MHSV (mass hourly space velocity)

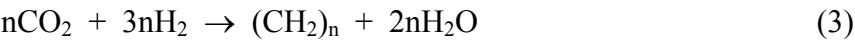
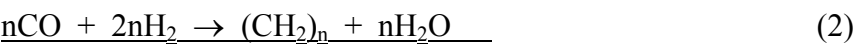
1. INTRODUCTION

As petroleum-derived fuels continue to dramatically increase in price, and world-wide future availability is in question, this scenario presents scientists with a unique challenge and an opportunity to develop new technologies to meet current and future energy demands.¹ These future technologies must minimize their impact on the environment, specifically carbon dioxide (CO₂) emissions.¹ Since CO₂ is readily available from the air, seawater, and as a byproduct of many industrial energy-producing processes that include gas, oil, and coal-fired power plants and conventional Fischer-Tropsch (FT) processes, it could serve as an abundant chemical feedstock for the production of energy-rich hydrocarbons similar to middle-distillate fuels.¹ Additionally, processes that utilize waste CO₂ from the environment could be envisioned as CO₂-neutral.²

The US Naval Research Laboratory (NRL) has recently reported developing a process to recover CO₂ from seawater.³⁻⁶ CO₂ is 140 times more concentrated in seawater than in air on a weight-per-volume basis (g/mL).² As this technology is currently being scaled and optimized, new and improved catalysts are being developed for the conversion of CO₂ to energy-rich hydrocarbons by NRL⁷⁻¹⁰ and others.¹¹⁻¹⁷ NRL's current research involves a two-step synthetic approach for producing liquid hydrocarbons from CO₂ and hydrogen (H₂).

In the first-step, CO₂ and H₂ are reacted over an iron-based catalyst to produce light olefins. The mechanism of CO₂ hydrogenation has been proposed to occur in two steps as shown in equations 1-2.^{9,11} The reverse water-gas shift (RWGS, Equation 1 below) is endothermic and

produces carbon monoxide (CO). This CO is then carried forward in an exothermic FT synthesis step (Equation 2), producing predominantly monounsaturated hydrocarbons (Equation 3). Carbon dioxide is also hydrogenated directly to methane, in a widely cited thermodynamically favorable and highly competitive side reaction (Equation 4).



The water formed in the primary reactions involved in CO₂ hydrogenation (Equations 1-4) and typical FT synthesis is known to negatively influence catalyst activity and product selectivity.¹⁸⁻²⁰

One objective of this study is to modify the catalyst surface with a silica-stabilized coating to prevent the water vapor produced in the reaction sequence (Equations 1 and 2) from negatively influencing catalyst activity by re-oxidation or accelerated crystallization of the metal oxide surface.²¹ By decreasing the effects of water vapor on the catalyst surface, the equilibrium at the catalyst surface should favorably shift to the production of desired intermediates such as olefins over intermediates such as CO or methane (Equations 1-3). Light olefins (C₂-C₆) produced from the reaction of CO₂ and H₂ may be further reacted in a second, sequential reactor by oligomerizing to higher linear olefins.²²⁻²⁴ The low temperature oligomerization of ethylene over Ni-exchanged amorphous silica-alumina (ASA) has been reported extensively by Heveling²⁵⁻²⁷ and others,^{28,29} where the reaction generates a product distribution selective for even-numbered

carbon oligomers (C₄-C₂₂).³⁰ As part of a second objective, data from the oligomerization of pure ethylene are reported as a model olefin for the development of new and improved ASA-supported nickel catalysts for the direct and selective oligomerization to higher molecular weight olefins in the second step of a two-step approach for producing liquid hydrocarbons from carbon dioxide and hydrogen. These higher hydrocarbons can be direct substitutes for crude oil-distilled middle-distillate fuels.

2. EXPERIMENTAL SECTION

2.1. Chemicals and Materials. Chemicals were reagent grade and were obtained from Aldrich Chemical Company, Milwaukee, WI and, unless noted otherwise, were used as received.

2.2. Catalyst Preparation. K/Mn/Fe on Al₂O₃ catalyst: K/Mn/Fe on γ -Al₂O₃ catalyst was prepared by incipient wetness impregnation (IWI) method, where Fe(NO₃)₃•9H₂O (327.7 g), KMnO₄ (92.2 g), and KNO₃ (13.9 g) were dissolved in boiling deionized water (0.5 L) and slowly poured over γ -Al₂O₃ (389.5 g, Matheson Coleman & Bell, surface area 218.3 m²/g, pore radius 1.2-3.7 nm, 80-200 mesh) until excess liquid was just observed, at which point the remaining metal salt solution was added. The mixture was slowly dried on a hotplate (80-90 °C) with frequent stirring until achieving a tacky dryness and then calcinated at 350 °C in a furnace for 87 h in air. *Caution! Make sure to prepare in well-ventilated hood as a large volume of NO₂ gas is released in the process.* The resulting dark maroon powder was collected and gently ground to remove visible clumps (yield = 506.4 g). A portion of the above K/Mn/Fe on Al₂O₃ catalyst was further functionalized with a silica layer by a method reported in the literature,²¹ where K/Mn/Fe on Al₂O₃ was impregnated with 9% weight silica by adding tetraethyl orthosilicate (TEOS) in hexane with stirring at room temperature. The catalyst is then dried

overnight prior to heating at 120 °C in static air for 2 hours. The final silica-coated K/Mn/Fe on Al_2O_3 was obtained by calcinating the sample at 540 °C for 4 hours.

Amorphous silica-alumina (ASA) particles: All ASA pellets were prepared by co-precipitating silica from TEOS and alumina from $\text{Al}(\text{NO}_3)_3 \cdot 9\text{H}_2\text{O}$ to target a 5% or 15% Al content by base-catalyzed hydrolysis using concentrated NH_4OH (28%) by titration. Hydrogels at specified pH values were obtained based on a modified literature procedure¹⁸ by monitoring the titration progress with a pH probe (Orion 4-Star pH-ISE Benchtop pH meter with Ross Ultra Rugged pH probe, 8104BNUWP) and then aging for 1 hour at 45 °C. The obtained hydrogel was then filtered and washed with deionized water prior to spreading the formed hydrogels onto perforated stainless-steel sheets (grade 304, hole diameter 0.045 inch, hole depth = 0.0178 inch). Upon baking in an oven at 110 °C for 1 hour, the ASA particles were obtained as small, white pellets.

Ni-exchanged amorphous silica-alumina (NiASA): The above ASA materials were further exchanged with nickel cations by an ion exchange protocol reported elsewhere.³¹ Each ASA sample was combined in a round-bottom flask with a 1 M solution of $\text{Ni}(\text{NO}_3)_2 \cdot 6\text{H}_2\text{O}$ in absolute ethanol (80 mL Ni solution per 6 grams ASA). While gently tumbling on a rotary evaporator at atmospheric pressure heated by an oil bath, each ASA sample was refluxed in the nickel solution for 4 hours prior to filtering and washing the particles several times with deionized water. The final NiASA particles were isolated and dried in an oven at 110 °C.

Calcinated ASA (ASAc) and Ni-exchanged calcinated ASA (NiASAc): Samples of the prepared ASA were calcinated under static air in a furnace set to 550 °C for 1 hour. Samples of calcinated ASA were exchanged with nickel cation following the same NiASA preparation described above. Additionally, a commercial ASA (Sigma-Aldrich, grade 135) was also utilized

as catalyst support, where Ni exchange and calcination procedures are similar to those described above.

2.3. Materials Characterization. Material properties of all ASA and NiASA (calcinated and uncalcinated) were characterized by x-ray photoelectron spectroscopy (XPS), microporosity measurement, field emission scanning electron microscopy (FESEM) and Fourier-transform infrared (FTIR) spectroscopy. XPS was used to assess the surface species and quantities present on the different ASA particles as well as commercial ASA using a K-Alpha instrument (Thermo Scientific, UK) with an instrument-specific powder sample holder, and Unifit (Version 2011, Revision F) software for data analysis. A monochromated Al K_{α} x-ray source was used, where the excitation energy was 1486.68 eV \pm 0.2, and the dwell time (0.05 s) and pass energy (200 eV) were also held constant. The binding energy (BE) range was viewed from -9.92 to +1350.08 eV, for a total of 1361 data points per analysis. Structural and chemical characterization was performed with a FESEM (Model LEO DSM 982, LEO) operated at an accelerating voltage between 5-10 kV, and the working distance varied from 8-12 mm.

Brunauer-Emmett-Teller (BET) surface areas were measured using a Micrometrics ASAP2010 accelerated surface area and porosimetry system. FTIR spectra were recorded for samples pressed in KBr pellets (1:100 sample to KBr weight ratio) and analyzed using OMNIC software (Thermo Electron Corporation, 2001) over the frequency range of 4000-400 cm^{-1} . Ni-exchanged ASA samples were submitted for elemental analysis, where percent Ni concentration was determined by inductively coupled plasma atomic emission spectroscopy (ICP-OES) analysis (Galbraith Laboratories, Inc., Knoxville, TN).

2.4. Carbon Dioxide Hydrogenation. A fixed-bed reactor (Figure 1) was prepared by loading a mixture of the K/Mn/Fe on $\gamma\text{-Al}_2\text{O}_3$ catalyst and $\gamma\text{-Al}_2\text{O}_3$ filler (17.82 g catalyst, 2.18 g alumina for 20.00 g total) in a stainless-steel tube (9 inches long, 1/2 inch OD, 3/8 inch ID),

drying with nitrogen (100 sccm, 265 psig, 300 °C), and finally reducing the catalyst with CO or H₂ (2 hours, 300 °C, 100 sccm). Once reduced, the reactor was purged with nitrogen for 1 hour prior to introducing the reactive gases, where flows were set by mass flow controllers (Sierra Instruments) at 100 sccm (25 sccm CO₂, 75 sccm H₂) with 10 sccm of nitrogen as an internal gas chromatography (GC) standard for a total flow of 110 sccm. The pressure of the system was maintained at 265 psig with a digital backpressure regulator (Alicat), and temperature was controlled across 3 zones of the reactor heated to 300 °C with 1-foot lengths of heating tape (Amptek) using K-type thermocouples and PID temperature controllers (Omega). Liquid products were collected in a high pressure reactor vessel (Parr) cooled to 5 °C with an immersion cooler (SP Scientific) in a water bath, and the product gas stream was first dried over a bed of 3 Å molecular sieves prior to GC analysis (Agilent Technologies). Each experimental sequence was set for a total of 5 GC sampling runs with 12 hour post-run intermission.

2.5 Ethylene Oligomerization. A fixed-bed reactor was prepared by loading a stainless steel tube (9 inch length, 1/2 inch OD, 3/8 inch ID) with variable amounts either commercial or particle-formed Ni-exchanged ASA with commercial ASA filler (~ 10 g total). The catalyst was dried with flowing nitrogen at 300 °C overnight prior to introducing compressed ethylene at a flow rate (10 sccm) controlled by mass flow controller (Sierra Instruments) where temperature was established at 120 °C across 3 zones using K-type thermocouples and PID controllers (Omega). Liquid products were trapped in a 500 mL sample storage cylinder (Swagelok) chilled in an acetone bath to -50 °C with an immersion cooler (SP Scientific), and the pressure of the system was maintained with a digital back-pressure regulator to 415 psig. Liquid products were analyzed by GC-MS (Agilent Technologies).

3. RESULTS AND DISCUSSION

3.1. Carbon Dioxide Hydrogenation. A catalyst formulation that has been previously well-characterized in a continuously-stirred tank reactor (CSTR) environment was used as the baseline catalyst to demonstrate the feasibility of using a silica-stabilized coating to enhance catalyst activity in a fixed-bed tubular reactor.^{9,21} In the initial studies, the baseline catalyst was reduced in the fixed-bed tubular reactor by carbon monoxide to form iron carbide phases on the catalyst. It has been proposed that these carbide phases are essential in FT synthesis for chain growth.³²⁻³⁴ This has been shown by changing the reducing agent of the fresh catalyst from CO to H₂, resulting in a lower CO conversion.³⁵ Table 1 provides the observed hydrogenation performance as CO₂ percent conversion and product distribution (CO and hydrocarbons) of the baseline catalyst reduced in CO. The reaction was run for over 116 hours. After the first 12 hours, CO₂ conversion remained steady between 31 and 35%. The hydrocarbon selectivity (not including methane) increased to as high as 65.4% of the CO₂ converted, where the olefin/paraffin ratio remained stable at 5.3. A shift toward higher hydrocarbon selectivity was observed as the C6+ fraction increased from 0 to 9.0% over the course of 116 hours. This is in agreement with pretreatment studies of Fe-based FTS catalysts that showed that CO reduction led to longer hydrocarbon chains and less methane production.³⁶ Higher activities were also achieved after a slower approach (e.g., 50 h) to reach steady-state conditions.³⁷ Such an increase in activity is suspected to be a result of the increased basicity of the carbide phase at the catalyst surface; enhancing the absorption and dissociation of CO while also decreasing the frequency of secondary hydration reactions for olefin products.³⁸ Approximately 2.4 mL of liquid hydrocarbon were collected in the trap after 116 hours.

Preliminary studies of iron catalyst modified with 9% TEOS and tested for 8 hours found that CO₂ conversion increased by as much as 22%.²¹ In addition, the selectivity towards CO and methane was shown to decrease. When 9% TEOS was added to the baseline catalyst used in the

present studies, Table 2 shows an 8.8% average decrease in overall CO₂ conversion after 12 hours as compared to the baseline catalyst. During this time the CO selectivity increased by as much as 31% and methane selectivity increased very little. The loss in CO₂ conversion and the higher selectivity of CO reduced the overall hydrocarbon selectivity in the C₂-C₆+ fraction. In addition, the selectivity within the C₂-C₆+ fraction shifted away from the formation of olefins as shown by a 30% decrease in the olefin to paraffin ratio over time.

Preliminary studies by Song, *et al.*²¹ report increases in CO₂ conversions by as much as 22% when H₂ was used as the reducing agent. The studies reported here include a comparison of CO to H₂ to elicit the role of the reducing agent on CO₂ conversion and hydrocarbon selectivity of the baseline catalyst and the modified catalyst. Table 3 provides the results of the baseline catalyst reduced in H₂. Comparing the baseline catalysts over time (Tables 1 and 3) shows the CO₂ conversion is not notably affected by the reducing agent. While CO selectivity increases by about 12% over the baseline catalyst reduced in H₂, the hydrocarbon selectivity and the olefin paraffin ratios remain similar for both baseline catalysts. In addition, Table 3 shows a 32% shift in hydrocarbon selectivity towards C₆+ over time. Indeed, 3.3 mL of liquid hydrocarbon was collected from the trap after 92 hours compared to 2.4 mL collected after 116 hours.

Table 4 provides the data collected for the modified catalyst reduced in H₂. Comparing the baseline catalyst and the modified catalyst reduced in H₂ (Tables 3 and 4) shows that the CO₂ conversion was reduced after the first 12 hours by an average of 21% overtime and methane selectivity increased by an average of 13% for the modified catalyst. A shift toward formation of more saturated hydrocarbons is observed over the modified catalyst as the average olefin to paraffin ratio after the first 12 hours is 4.4 compared to 5.3 for the baseline catalyst. In addition the overall selectivity of C₂-C₆+ is reduced on average 24% by the modification of the catalyst.

Comparing the modified catalyst reduced in CO and H₂ (Tables 2 and 4) shows that the modified catalyst reduced in H₂ has much greater selectivity towards olefins than the modified catalyst reduced in CO. It also produces 10% less CO over time. However, the modified catalyst in H₂ has the lowest average CO₂ conversion over time compared to the other catalyst and conditions.

In Tables 1-4, yield is calculated by multiplying the C2-C6+ hydrocarbon selectivity values with the CO₂ conversion values. Tables 1 and 3 show that on average after 12 hours the C2-C6+ yield is 21% on a carbon basis. This means an average of 21% of CO₂ fed into the reactor is converted to C2-C6+ molecules. This average yield of 21% for both baseline catalysts is significantly higher than the 17% and 16% yield obtain for the modified catalysts. Clearly the addition of TEOS to the catalysts negatively affects the transport of species to the catalyst sites.

The total hydrocarbon product distribution as a function of time and catalyst modification can be described by means of Anderson-Schulz-Flory (ASF) growth distribution plots, where $\ln(W_N/N)$ (W_N is the weight fraction of HC containing N number of carbon atoms) is plotted as a function of carbon number (N). The chain growth probability α is inferred by the slope.³⁹ Tables 1 through 4 show on average the chain-growth probability for each catalyst condition reaches its maximum after 60 hours. Tables 1 and 4 show that while the average CO₂ conversion was reduced by the addition of TEOS to the baseline catalyst, the average chain-growth probability after 12 hours increased slightly from 0.48 to 0.52 when the catalyst was reduced by CO. When the baseline catalyst was reduced in H₂ compared to reduction by CO the average chain-growth probability increased from 0.48 to 0.54. This appears to be the result of a shift in hydrocarbon selectivity towards C6+ from an average of 6% (Table 1, catalyst reduced by CO) to 9% (Table 3, catalyst reduced by H₂). The average higher chain-growth probability for catalyst reduced by H₂ was not affected by the modification of the catalyst with TEOS. The Tables indicate that

under the fixed-bed reaction conditions for CO₂ hydrogenation, reduction with CO is favored for the production of light (< C₆) olefins.

3.2 Ethylene Oligomerization □ Catalyst Characterization. Amorphous silica-aluminas (ASAs) offer a robust catalyst platform that may be systematically tailored by controlling pore size distribution,⁴⁰⁻⁴² degree of crystallinity,⁴³ and number and strength of Brønsted and Lewis acidic sites⁴⁴ to optimize catalytic performance. Specifically, these catalysts are notably effective in oligomerization of propylene and butylene. Although previously reported results have established a foundation from which to approach the use of ASA supports for catalysis, there remains a challenge in tuning their properties to achieve specific hydrocarbon selectivity such as 1-hexene or a particular hydrocarbon region such as C₉-C₁₆.

In this study hydrogels were synthesized by co-precipitating aluminum and silica. By systematically altering the synthesis as a function of aluminum content and pH, a set of support materials were generated (Table 5). The ASA supports were formed into particles by heating the gel to 110 °C within molds of a specified size, and nickel was loaded onto the resultant pelletized materials by ion exchange.⁴⁵ The catalysts were initially characterized by XPS, FT-IR, BET and elemental analysis to identify changes in ASA composition as a function of proportion of used Si and Al precursors, pH of hydrogel isolation, nickel cation exchange, and calcination conditions. The synthesized ASA and NiASA particle characterization data are provided in Figure 2, where it was observed that the SiO₂/Al₂O₃ ratio increased with pH during hydrogel formation for 5% Al-containing ASA and less notably so for the 15% Al-containing ASA. The observed higher Al surface concentration for calcinated samples is also supported by the expected increase in SiO₂/Al₂O₃ ratio for calcinated samples reported in the literature.⁴⁶

With regards to Ni loading, elemental analysis indicates that there was a decreased Ni concentration for calcinated ASA when compared with uncalcinated ASA (Table 5). This was likely due to the depletion of surface silanol groups by dehydration that may be essential for Ni coordination.⁴⁷ Also, it was found that in general ASA with higher Al content contained higher concentrations of Ni. As it has been suggested that Al-OH-Si bridging hydroxyl groups are Ni-exchangeable sites in ASA-supported Ni catalysts,^{36,48} it followed that an increase in Al content would result in higher Ni loading. Indeed the FT-IR spectra of the Ni-loaded ASAs were identical to those of their Ni-free precursors, with the exception of a diminishing intensity in the broad silanol stretch at 3450 cm⁻¹. We did not identify any particular trends in the degree to which the silanol band had diminished, and the conditions under which the ASA support materials were originally synthesized. However, we did generally find that the degree to which the silanol band diminished was less for the calcinated ASAs than for non-calcinated ASAs. This qualitatively indicates that the calcinated ASAs are less capable of loading Ni, probably due to a lower concentration of surface silanols. This hypothesis was supported by elemental analysis. Additionally, the calcinated ASAs were determined to have over a 30% loss in surface area by BET.

3.3. Ethylene Oligomerization □ Catalyst Performance. In this study, pure ethylene was used as a model to test the optimization of well-characterized ASA-supported nickel catalysts for the selective oligomerization of olefins to higher molecular weight hydrocarbons in the C9-C16 region. The ASA characterization shown in Table 5 verified that the uncalcinated supports contained higher nickel loading and greater surface area. In this evaluation, 20 grams of uncalcinated, nickel-loaded ASA support synthesized using 5% Al at pH 5.71 (Sample 1, Table 5) was explored at different mass hourly space velocities (MHSV) to determine conditions needed to achieve high ethylene conversion as well as ideal product selectivity (C9-C16 olefins

for fuel application). Figure 3 shows ethylene conversion and the mass percent selectivity for hydrocarbon chain length as a function of MHSV at 415 psig. The Figure shows that as MHSV was decreased from 1.10 to 0.16 h⁻¹ and ethylene conversion increased from 33% to 64%. The remaining 67% to 36% of the ethylene was not converted. In addition, hydrocarbon fraction detected in the C9-C16 region increased from 52% to 86%. This observation was supported by literature reports, where increasing the retention time of reactant ethylene feed on the catalyst bed resulted in a lower MHSV value, allowing for further chain growth of the formed oligomer.⁴⁹

4. CONCLUSIONS

The separate steps of CO₂ hydrogenation and ethylene oligomerization were explored to identify and improve catalyst composition and reaction conditions ideal for scale-up considerations. Initial results for CO₂ hydrogenation demonstrated a loss in conversion and hydrocarbon selectivity to olefins by the modification of a Fe/Mn/K catalyst supported on alumina with TEOS under fixed-bed conditions. Further, the results indicated that, under fixed-bed reaction conditions for CO₂ hydrogenation, the Fe/Mn/K catalyst produced lighter olefins in greater quantities when CO was used as the reducing agent.

Characterization of ASA formed under conditions of different Al content, pH of synthesis, and calcination treatment indicated that the structure of ASA supports can be directed to control Ni catalyst loading as well as the surface silica/alumina ratio. Preliminary tests indicated that the formed NiASA performed well as a catalyst for the oligomerization of ethylene, where ethylene conversion as well as selectivity for oligomers of higher chain length were successfully targeted by decreasing the MHSV. As such, the pelletized NiASA are considered as potential catalysts for the upgrading of light olefins from an initial CO₂ hydrogenation reactor to higher olefins of jet fuel-specific composition when used in either a merged or separated oligomerization stage

reactor. These results indicate promising directions for conditions and catalyst compositions to use in the scale-up demonstration of CO₂-to-fuel conversion, where there is ongoing work to improve reactor design, catalyst compositions, as well as reaction and process conditions (e.g., CO₂ hydrogenation in a single-step to liquid olefins).

AUTHOR INFORMATION

Corresponding Author

*Telephone: +01-202-767-2673. E-mail: Heather.Willauer@nrl.navy.mil

ACKNOWLEDGEMENTS

This work was supported by the Office of Naval Research both directly and through the Naval Research Laboratory.

REFERENCES

- (1) Olah, G. A.; Goeppert, A.; Prakash, G.K.S. *Beyond Oil and Gas: The Methanol Economy*; Wiley-VCH Verlag GmbH & Co.: Weinheim, 2006.
- (2) Coffey, T.; Hardy, D. R.; Besenbruch, G. E.; Schultz, K. R.; Brown, L. C.; Dahlburg, J. P. *Defense Horizons* **2003**, *36*, 1.
- (3) Willauer, H. D.; Hardy, D. R.; Lewis, M. K.; Ndubizu, E. C.; Williams, F. W. *Energy Fuels* **2009**, *23*, 1770-1774.
- (4) Willauer, H. D.; Hardy, D. R.; Lewis, M. K.; Ndubizu, E. C.; Williams, F. W. *J. Phys. Chem. A* **2010**, *114*, 4003-4008.
- (5) Willauer, H. D.; Hardy, D. R.; Lewis, M. K.; Ndubizu, E. C.; Williams, F. W. *Energy Fuels* **2010**, *24*, 6682-6688.
- (6) Willauer, H. D.; DiMascio, F.; Hardy, D. R.; Lewis, M. K.; Williams, F. W. *Ind. Eng. Chem. Res.* **2011**, *50*, 9876-9882.
- (7) Dorner, R. W.; Hardy, D. R.; Williams, F. W.; Davis, B. H.; Willauer, H. D. *Energy Fuels* **2009**, *23*, 4190-4195.
- (8) Dorner, R. W.; Hardy, D. R.; Williams, F. W.; Willauer, H. D. *Catal. Commun.* **2010**, *11*, 816-819.
- (9) Dorner, R. W.; Hardy, D. R.; Williams, F. W.; Willauer, H. D. *Appl. Catal., A* **2010**, *373*, 112-121.
- (10) Dorner, R. W.; Hardy, D. R.; Williams, F. W.; Willauer, H. D. *Catal. Commun.* **2011**, *15*, 88-99.

- (11) Riedel, T.; Schaub, G.; Jun, K. -W.; Lee, K. -W. *Ind. Eng. Chem. Res.* **2001**, *40*, 1355-1363.
- (12) Ning, W.; Koizumi, N.; Yamada, M. *Energy Fuels* **2009**, *23*, 4696-4700.
- (13) Pan, Y. -X.; Liu, C. -J.; Ge, Q. *Catal.* **2010**, *272*, 227-234.
- (14) Dorner, R. W.; Hardy, D. R.; Williams, F. W.; Willauer, H. D. *Energy Environ. Sci.* **2010**, *3*, 884-890.
- (15) Wang, W.; Wang, S.; Ma, X.; Gong, J. *Chem. Soc. Rev.* **2011**, *40*, 3703-3727.
- (16) Centi, G.; Iaquaniello, G.; Perathoner, S. *ChemSusChem* **2011**, *4*, 1265-1273.
- (17) Quadrelli, E. A.; Centi, G.; Duplan, J. L.; Perathoner, S. *ChemSusChem* **2011**, *4*, 1194-1215.
- (18) Wu, J.; Saito, M.; Takeuchi, M.; Watanabe, T. *Appl. Catal., A* **2001**, *218*, 235-240.
- (19) Botes, F. G. *Catal. Rev.* **2008**, *50*, 471-491.
- (20) Baya, M.; Rahimpour, M. R. *J. Nat. Gas Sci. Eng.* **2012**, *9*, 73-85.
- (21) Ding, F.; Zheng, B.; Song, C.; Guo, X. *Prep. Pap.-Am Chem. Soc. Div. Fuel Chem.* **2012**, *57*, 444.
- (22) Jarallah, A. M. A. *J. Catal.* **1992**, *14*, 1-124.
- (23) Olah, G. A.; Molinár, A. Oligomerization and Polymerization. In *Hydrocarbon Chemistry (2nd Ed.)*; Wiley and Sons, Inc.: New Jersey, 2003, pp. 723-806.
- (24) de Klerk, A. *Energy Fuels* **2006**, *20*, 1799-1805.
- (25) Heveling, J.; Nicolaides, C. P.; Scurrrell, M. S. *Appl. Catal., A* **1998**, *173*, 1-9.
- (26) Heveling, J.; Nicolaides, C. P.; Scurrrell, M. S. *Catal. Lett.* **2004**, *95*, 87-91.
- (27) Heveling, J.; Nicolaides, C. P. *Catal. Lett.* **2006**, *107*, 117-121.
- (28) Heydenrych, M. D.; Nicolaides, C. P.; Scurrrell, M. S. *J. Catal.* **2001**, *197*, 49-57.
- (29) Lallemand, M.; Finiels, A.; Fajula, F.; Hulea, V. *J. Phys. Chem. C* **2009**, *113*, 20360-20364.
- (30) Heveling, J.; Nicolaides, C. P.; Scurrrell, M. S. *Chem. Commun.* **1991**, 126-127.
- (31) Hensen, E. J. M.; Poduval, D. G.; Magusin, P. C. M. M.; Coumans, A. E.; van Veen, J. A. R. *J. Catal.* **2010**, *269*, 201-218.
- (32) Shroff, M. D.; Kalakkad, D. S.; Coulter, K. E.; Kohler, S. D.; Harrington, M. S.; Jackson, N. B.; Sault, A. G.; Datye, A. K. *J. Catal.* **1995**, *156*, 185-207.
- (33) Li, S. Z.; Krishnamoorthy, S.; Li, A. W.; Meitzner, G. D.; Iglesia, E. *J. Catal.* **2002**, *206*, 202-217.
- (34) Herranz, T.; Rojas, S.; Perez-Alonso, F. J.; Ojeda, M.; Terreros, P.; Fierro, J. L. G. *J. Catal.* **2006**, *243*, 199-211.
- (35) Bukur, D. B.; Nowicki, L.; Manne, R. K.; Lang, X. S. *J. Catal.* **1995**, *155*, 366-375.
- (36) Bukur, D. B.; Nowicki, L.; Patel, S. A. *Can. J. Chem. Eng.* **1996**, *74*, 399-404.
- (37) Bukur, D. B.; Lang, X.; Ding, Y. *Appl. Catal., A* **1999**, *186*, 255-275.
- (38) Zhang, J. -L.; Ma, L. -H.; Fan, S. -B.; Zhao, T. -S.; Sun, Y. -H. *Fuel* **2013**, 116-123.
- (39) Ma, W. -P.; Zhao, Y. -L.; Li, Y. -W.; Xu, Y. -Y.; Zhou, J. -L. *React. Kinet. Catal. Lett.* **1999**, *66*, 217-223.
- (40) Snel, R. **1987**, *33*, 281-294.
- (41) Carati, A.; Ferraris, G.; Guidotti, M.; Moretti, G.; Psaro, R.; Rizzo, C. *Catal. Today* **2003**, *77*, 315-323.
- (42) Vít, Z.; Šolcová, O. *Microporous Mesoporous Mater.* **2006**, *96*, 197-204.
- (43) Nicolaides, C. P. *Appl. Catal., A* **1999**, *185*, 211-217.

- 1
2
3
4
5
6
7
8
9
10
11
12
13
14
15
16
17
18
19
20
21
22
23
24
25
26
27
28
29
30
31
32
33
34
35
36
37
38
39
40
41
42
43
44
45
46
47
48
49
50
51
52
53
54
55
56
57
58
59
60
- (44) Bartoszek, M.; Eckelt, R.; Jäger, C.; Kosslick, H.; Pawlik, A.; Schulz, A. *J. Mater. Sci.* **2009**, *44*, 6629-6636.
- (45) Heveling, J.; Nicolaides, C. P.; Scurrall, M. S. *J. Chem. Soc., Chem. Commun.* **1991**, 126-127.
- (46) Pieta, I. S.; Ishaq, M.; Wells, R. P. K.; Anderson, J. A. *Appl. Catal., A* **2010**, *390*, 127-134.
- (47) Crepau, G.; Montillout, V.; Vjmont, A.; Arieu, L.; Cseri, T.; Maugé, F. *J. Phys. Chem. B* **2006**, *110*, 15172-15185.
- (48) Burwell, Jr., R. L. *Chemtracts* **1991**, *July/August*, 242-244.
- (49) de Klerk, A.; Engelbrecht, D. J.; Boikanyo, H. *Ind. Eng. Chem. Res.* **2004**, *43*, 7449-7455.